

ON DEVELOPING ALTERNATING VOLTAGE AROUND A ROTATING CIRCULAR RING UNDER PLANE WAVE EXCITATION IN THE PRESENCE OF AN ECCENTRICALLY POSITIONED METALLIC CORE

C. A. Valagiannopoulos

School of Electrical and Computer Engineering
National Technical University of Athens (NTUA)
GR 157–73, Zografou, Athens, Greece

Abstract—Rotating coils constitute a type of electrical transformers used to produce alternating voltage pulses exploiting the phenomenon of electromagnetic induction. In this study, we investigate the influence of the electromagnetic scattering from a metallic obstacle located inside the moving component. In particular, a perfectly conducting spherical core is positioned eccentrically inside a thin circular ring, rotating around an arbitrary axis passing through its own center, under plane wave excitation. Methods and formulas implemented in scattering and induction problems have been utilized for the derivation of the developed potential difference around the loop. Several graphs of the voltage output versus the geometrical characteristics of the configuration, are shown and explained.

1. INTRODUCTION

It is common knowledge that the electromagnetic induction is the production of voltage across a conductor situated in a changing magnetic field or a conductor moving through a stationary magnetic field. Many studies have been published concerning analyses and applications on such a phenomenon. In [1], a time stepping two-dimensional FEM is performed for modeling and analysis of an induction machine where the technique is used for the magnetic field calculation, and for the vector potential derivation of the machine. In addition, Sun and Nie have illustrated the capabilities of a flexible numerical approach to study the multicomponent induction response in anisotropic formations involving eccentric tools, while dipping beds are

Corresponding author: C. A. Valagiannopoulos (valagiannopoulos@gmail.com).

included to demonstrate the flexibility of the method [2]. Furthermore, the negative effect of the induction from high power microwaves on integrated circuits has been examined in [3], where three kinds of destructions are also investigated.

The electromagnetic scattering is defined as the modification of the incident field in the presence of an obstacle through the fulfillment of the boundary conditions. Numerous treatises have been performed on this issue, especially related to scattering by spherical obstacles whose shape is susceptible to analytical solutions. For example, the problem of the electrical current distribution along thin radial impedance monopole, located on the perfectly conducting sphere, has been solved in a rigorous electrodynamic formulation [4]. In [5], the point-source scattering by an electrically large conducting sphere is discussed, where Bessel functions of complex order are utilized. Moreover, the scattering cross section of a spherical obstacle constructed from a medium that gives effective doubly-negative permittivity and permeability, has been rigorously derived [6]. Finally in [7], a simplified solution is obtained to the problem of a circular wire flown by arbitrary current radiating in the presence of a metallic core.

In this work, we combine the two aforementioned issues (induction and scattering), by considering a structure comprised of a rotating thin circular loop and an eccentrically positioned metallic spherical scatterer, illuminated by a plane wave. The rotation happens around an arbitrary axis passing through the center of the spherical cavity. The magnetic vector potential at the position of the thin closed wire, is evaluated with use of spherical eigenfunction expansions and through the enforcement of the boundary conditions. The time rate of change of magnetic flux is computed from the line integral of the electric field around the metallic coil. The presence of the sphere, modifies the direction of the magnetic field and implicitly the magnetic flux through the ring, an influence which has not been studied yet. The DC offset and the RMS value of the produced voltage are represented in several graphs with respect to the size of the sphere, the rotation axis and the excitation/rotation frequencies as well. By inspection of the variations, one can reach various useful and applicable conclusions.

2. MATHEMATICAL FORMULATION

2.1. Device Configuration

The physical configuration of the inspected problem is shown in Fig. 1(a), where the spherical (unprimed) coordinate system (r, θ, ϕ) and the equivalent Cartesian one (x, y, z) are also defined. The origin O coincides with the center of a perfectly conducting sphere of radius

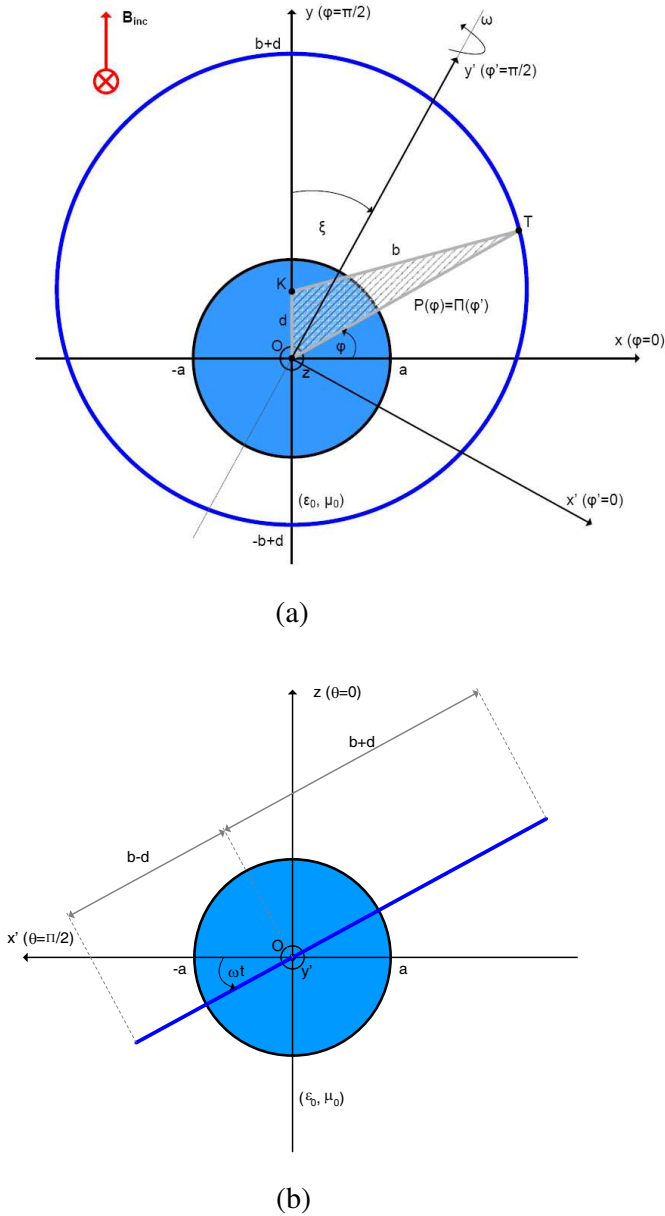


Figure 1. The physical configuration of the examined device as viewed from: (a) the positive z semi axis, (b) the positive y' semi axis.

a posed into vacuum (intrinsic parameters: ϵ_0, μ_0). A thin circular metallic wire of radius $b > a$ is shown on the x - y plane, with its center K at $(x, y, z) = (0, d, 0)$ posed eccentrically to the spherical core. This ring is rotated with respect to the axis $\phi = \pi/2 - \xi$ (on the plane $z = 0$) with circular frequency ω , in the presence of an x -polarized plane wave \mathbf{E}_{inc} (magnetic field \mathbf{B}_{inc} with sole y direction), with magnitude Q (in V/m), advancing towards the negative z semi-axis. Mind that the harmonic time dependence of the incident field, is of the form $\exp(-i\omega_0 t)$, possessing its own circular frequency ω_0 . Another (primed) coordinate system is additionally shown in Fig. 1(a) which is obtained by turning clockwise the unprimed one around z axis (which is common for both systems) by the angle ξ . In this way, the y' axis coincides with the rotating axis of the ring. In Fig. 1(b), we present a side view of the device as appeared from the positive y' semi-axis, when the frame is rotated by angle ωt , at an arbitrary time t .

2.2. Curve Parametrization for $\xi = 0$

The polar radius $P(\phi)$ of the eccentric circular loop at $t = 0$ (Fig. 1(a)), is determined by applying the law of cosines to the shaded triangle (OKT), where T is the representative point of the ring, yielding to:

$$P(\phi) = d \sin \phi + \sqrt{b^2 - d^2 \cos^2 \phi}. \quad (1)$$

Let us extract the parametric equation set of the rotated coil denoted by $\{x = \chi(\phi, t), y = \psi(\phi, t), z = \zeta(\phi, t)\}$, at the arbitrary time t when $\xi = 0$. The azimuthal angle $\phi \in [0, 2\pi)$ will play the role of the parametric variable even when the rotated closed wire does not belong exclusively to x - y plane. As the closed wire is rotated with respect to y axis, the corresponding coordinate $\psi(\phi, t)$ will be fixed, independent from the angle ωt and equal to $P(\phi) \sin \phi$. The rest two equations are derived by projecting the other edge of length $P(\phi) \cos \phi$, which is posed at angle ωt , upon the axes x and z . Accordingly, one obtains the following expressions:

$$\chi(\phi, t) = P(\phi) \cos \phi \cos \omega t, \quad (2a)$$

$$\psi(\phi, t) = P(\phi) \sin \phi, \quad (2b)$$

$$\zeta(\phi, t) = -P(\phi) \cos \phi \sin \omega t. \quad (2c)$$

The negative sign in (2c), is explained by inspection of Fig. 1(b).

2.3. Curve Parametrization for $\xi \neq 0$

In order to find the parametric equation of the curve when $\xi \neq 0$, we use the primed coordinate system. The polar equation of the

loop is now given by $\Pi(\phi') = P(\phi' - \xi)$, while the two azimuthal angles are connected obviously via the relation $\phi' = \phi + \xi$. Therefore, we take the formulas (2a)–(2c) replacing P by Π and the unprimed variables $\{\chi, \psi, \zeta, \phi\}$ by the primed ones $\{\chi', \psi', \zeta', \phi'\}$. In this sense, the parametric set of the primed coordinates with respect to unprimed azimuthal angle ϕ (after trivial algebraic manipulations), is written as follows:

$$\chi'(\phi, t) = P(\phi) \cos(\phi + \xi) \cos \omega t, \tag{3a}$$

$$\psi'(\phi, t) = P(\phi) \sin(\phi + \xi), \tag{3b}$$

$$\zeta'(\phi, t) = -P(\phi) \cos(\phi + \xi) \sin \omega t. \tag{3c}$$

The parametric equations of the arbitrarily rotated wire loop expressed in the unprimed coordinate system are denoted by $\{x = X(\phi, t), y = Y(\phi, t), z = Z(\phi, t)\}$ and are determined from the transformation relation below [8]:

$$\begin{bmatrix} X(\phi, t) \\ Y(\phi, t) \\ Z(\phi, t) \end{bmatrix} = \begin{bmatrix} \cos \xi & \sin \xi & 0 \\ -\sin \xi & \cos \xi & 0 \\ 0 & 0 & 1 \end{bmatrix} \cdot \begin{bmatrix} \chi'(\phi, t) \\ \psi'(\phi, t) \\ \zeta'(\phi, t) \end{bmatrix}. \tag{4}$$

If terms of the unprimed spherical coordinate system, the parametric representation of the arbitrarily rotated ring is constituted by the following equations:

$$R(\phi, t) = \sqrt{X^2(\phi, t) + Y^2(\phi, t) + Z^2(\phi, t)}, \tag{5a}$$

$$\Theta(\phi, t) = \arccos \left[\frac{Z(\phi, t)}{R(\phi, t)} \right], \tag{5b}$$

$$\Phi(\phi, t) = \arctan \left[\frac{Y(\phi, t)}{X(\phi, t)} \right]. \tag{5c}$$

Note that the distance of an arbitrary point from the origin remains constant throughout the rotation procedure equal to $P(\phi)$.

2.4. Electromagnetic Induction

According to Faraday’s law of induction [9], the induced voltage across a closed metallic wire (W) is defined as the line integral of the local electric field around the loop. In case of a monochromatic electric field with circular frequency ω_0 , the related formula is given below:

$$U = \Re \left[e^{-i\omega_0 t} \int_{(W)} \mathbf{E} \cdot d\mathbf{w} \right]. \tag{6}$$

It should be stressed that \mathbf{E} does not denote the real, time-dependent quantity, but the corresponding complex phasor. In case the field

quantities are expressed in terms of the unprimed spherical coordinate system, the Cartesian components are given by [10]:

$$\begin{bmatrix} E_x(r, \theta, \phi) \\ E_y(r, \theta, \phi) \\ E_z(r, \theta, \phi) \end{bmatrix} = \begin{bmatrix} \cos \phi \sin \theta & \cos \phi \cos \theta & -\sin \phi \\ \sin \phi \sin \theta & \sin \phi \cos \theta & \cos \phi \\ \cos \theta & -\sin \theta & 0 \end{bmatrix} \cdot \begin{bmatrix} E_r(r, \theta, \phi) \\ E_\theta(r, \theta, \phi) \\ E_\phi(r, \theta, \phi) \end{bmatrix}. \quad (7)$$

Once these functions are determined, the line integral of (6), is particularized to give [11]:

$$U(t) = \Re \left[e^{-i\omega_0 t} \int_0^{2\pi} (e_x(\phi, t)X_\phi(\phi, t) + e_y(\phi, t)Y_\phi(\phi, t) + e_z(\phi, t)Z_\phi(\phi, t)) d\phi \right], \quad (8)$$

where subscript ϕ corresponds to the azimuthal partial derivative of the related function. The small- e functions $\{e_x, e_y, e_z\}$ are the electric field components evaluated around the moving circular loop:

$$e_x(\phi, t) = E_x(R(\phi, t), \Theta(\phi, t), \Phi(\phi, t)), \quad (9a)$$

$$e_y(\phi, t) = E_y(R(\phi, t), \Theta(\phi, t), \Phi(\phi, t)), \quad (9b)$$

$$e_z(\phi, t) = E_z(R(\phi, t), \Theta(\phi, t), \Phi(\phi, t)). \quad (9c)$$

Thus, the only prerequisite to apply expression (8) and compute the induced voltage, is the explicit form of the total electric field in unprimed spherical coordinates.

2.5. Electromagnetic Scattering

The electric field into vacuum is comprised of the incident and the scattering component $\mathbf{E} = \mathbf{E}_{inc} + \mathbf{E}_{scat}$, where $\mathbf{E}_{inc} = \mathbf{x}Qe^{-ik_0z}$ and $k_0 = \omega_0\sqrt{\epsilon_0\mu_0}$. It is computed with use of spherical eigenfunctions and the following series expansion [12]:

$$e^{-ik_0r \cos \theta} = \sum_{n=1}^{+\infty} (-i)^{n+1} (2n+1) P_{0n}(\theta) j_n(k_0r). \quad (10)$$

The symbol $P_{mn}(\theta)$ corresponds to the Legendre function of degree n , order m and argument $\cos \theta$. The n th order spherical Bessel $j_n(x)$ and the spherical Hankel of the first kind $h_n(x)$, are also well-known [13]. Once the boundary condition at $r = a$ is imposed, the respective scattering components of the electric field are given by:

$$E_{r,scat}(r, \theta, \phi) = -Q \cos \phi \sum_{n=1}^{+\infty} L(n) P_{1n}(\theta) \frac{h_n(k_0r)}{k_0r}, \quad (11a)$$

$$E_{\theta,scat}(r, \theta, \phi) = -Q \cos \phi \cdot \sum_{n=1}^{+\infty} \left[\frac{J(n)}{n(n+1)} \frac{P_{1n}(\theta)}{\sin \theta} h_n(k_0 r) + \frac{L(n)}{n(n+1)} \frac{dP_{1n}(\theta)}{d\theta} \frac{h_n^d(k_0 r)}{k_0 r} \right], \quad (11b)$$

$$E_{\phi,scat}(r, \theta, \phi) = Q \sin \phi \cdot \sum_{n=1}^{+\infty} \left[\frac{J(n)}{n(n+1)} \frac{dP_{1n}(\theta)}{d\theta} h_n(k_0 r) + \frac{L(n)}{n(n+1)} \frac{P_{1n}(\theta)}{\sin \theta} \frac{h_n^d(k_0 r)}{k_0 r} \right], \quad (11c)$$

where:

$$J(n) = i^n (2n+1) \frac{j_n(k_0 a)}{h_n(k_0 a)}, \quad L(n) = (-i)^{n+1} (2n+1) \frac{j_n^d(k_0 a)}{h_n^d(k_0 a)}. \quad (12)$$

The Riccati functions are defined as $z_n^d(x) = d[xz_n(x)]/dx$, where $z_n(x)$ can be the spherical Bessel or Hankel function.

3. NUMERICAL RESULTS

3.1. Parameter Selection

Before presenting the numerical results, one should clarify the value ranges of the input parameters for our consideration. The rotation frequency of the loop and the oscillating frequency of the incident plane wave are both chosen within the interval: $\omega, \omega_0 \in 2\pi[1, 200]$ rad/sec, typically equal to $\omega, \omega_0 = 200\pi$ rad/sec. The radius of the rotating ring varies from 0.5 m to 2 m, usually close to $b = 1$ m. The rotation axis covers the entire plane $0 < \xi < \pi$, while in most cases is taken equal to $\xi = \pi/4$. The amplitude of the plane wave Q is not a crucial parameter and therefore is chosen high enough to give realistic values for the output voltages. It should be noted that the series in (11) are evaluated by truncation; in particular, we keep only the first $(N + 1)$ terms. The integer N is chosen proportional to the electrical size of the scatterer $|k_1|a$, in order to achieve convergence with maximum permissible error of 0.001%. Instead of the radius of the sphere, we use the normalized parameter $\frac{a}{b-a} \in [0, 1]$ as the core should be kept internal to the rotating ring. The eccentricity ratio $\frac{d}{b-a} \in [0, 1]$ is also utilized to quantify the relative transposition of the scatterer. In the following graphs, two quantities are mainly represented; the DC offset and the RMS value of the induced voltage, defined below:

$$U_{dc} = \frac{\omega}{2\pi} \int_0^{\frac{2\pi}{\omega}} U(t) dt, \quad U_{rms} = \sqrt{\frac{\omega}{2\pi} \int_0^{\frac{2\pi}{\omega}} [U(t) - U_{dc}]^2 dt}. \quad (13)$$

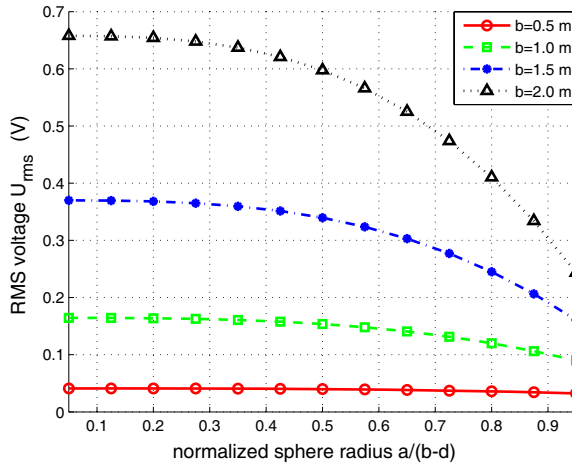


Figure 2. The RMS value of the induced voltage U_{rms} as function of the normalized radius of the sphere $\frac{a}{b-d}$ for various radii of the ring b . Plot parameters: $d = 0.2$ m, $\xi = \pi/4$ rad, $\omega_0 = 200\pi$, rad/sec, $\omega = 200\pi$ rad/sec, $Q = 10^5$ V/m.

3.2. Diagrams Discussion

In Fig. 2, the RMS component of the produced voltage is shown as function of the normalized sphere radius with constant position of the spherical scatterer d for several sizes of the rotating loop. The maximum magnetic flux through the circular wire (and implicitly the induced voltage) is proportional to the size of this ring. Note also that the normalized radius of the loop plays rather unimportant role when it is kept low. On the contrary, when the scatterer gets close to the frame, there is a diminishing effect on the measured quantity, which gets more significant for larger loops. This could be anticipated because an enlarged sphere decreases the available area for the magnetic field vector to pass through.

In Fig. 3, we display the variation of the RMS induced voltage with respect to the eccentricity ratio, with fixed size of the sphere a , for various radii of the ring. We do not show the curves for $\frac{d}{b-a} < 0.9$ because they exhibit a remarkable stability which verifies the unimportance of the eccentricity ratio when it possesses moderate magnitudes. However, substantial increase has been observed in case $\frac{d}{b-a} \rightarrow 1$, which means that the asymmetry of the structure has a crucially positive influence on the measured response. The negligible variation for $b = 0.5, 1$ m is attributed to the little available

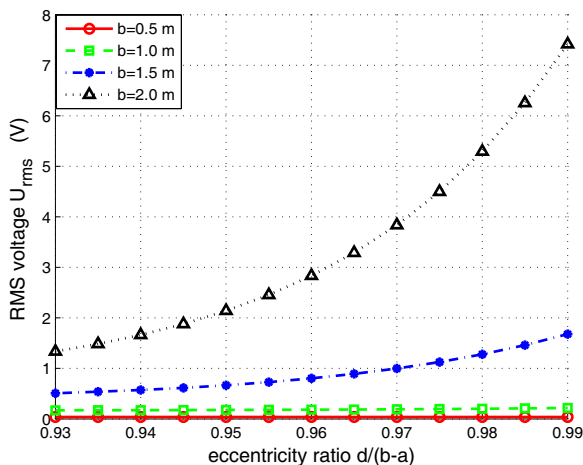


Figure 3. The RMS value of the induced voltage U_{rms} as function of the eccentricity ratio $\frac{d}{b-a}$ for various radii of the ring b . Plot parameters: $a = 0.2$ m, $\xi = \pi/4$ rad, $\omega = 200\pi$ rad/sec, $\omega_0 = 200\pi$ rad/sec, $Q = 10^5$ V/m.

manoeuvring room for the sphere when its radius is comparable to the size of the ring. In other words, the same change in eccentricity ratio, corresponds to lesser difference in the shape of the structure when b is chosen small enough.

In Fig. 4, the RMS value of the developed voltage around the loop, is represented as function of the rotation angle for several normalized radii of the sphere. One can notice that the waveforms are symmetric with respect to $\xi = \pi/2$, which is sensible because two complementary axes ξ are only diverse in the rotation direction, not affecting the measured quantity. When $\xi = 0, \pi$, the magnetic flux through the circular frame is null and therefore the produced voltage vanishes. The optimal result is achieved for $\xi = \pi/2$ where the amplifying effect of the eccentricity (same b, d and smaller a leads to less symmetric configurations) is rendered more obvious.

In Fig. 5(a), the RMS component of the produced voltage is shown in a contour plot with respect to the rotation frequency of the loop and the oscillation frequency of the incident plane wave. For increasing ω_0 , the recorded quantity gets reinforced with a pace negatively related to ω . Once the rotation frequency gets larger, there is either a stability in the measured output (modest ω_0) or a magnitude boost (substantial ω_0). It should be also remarked that when ω is very low, rapid variations in U_{rms} are observed for little change of ω_0 .

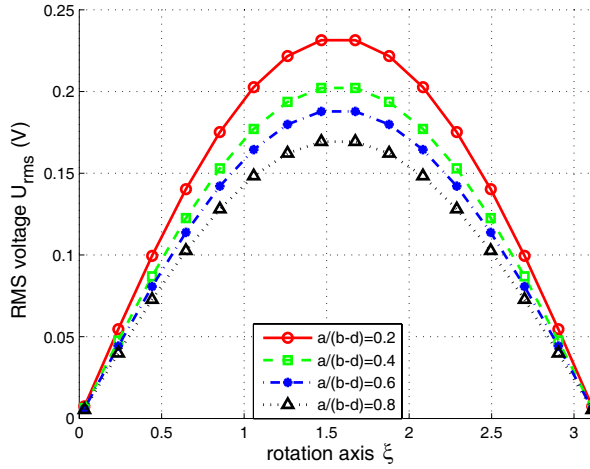


Figure 4. The RMS value of the induced voltage U_{rms} as function of the rotation angle ξ for several normalized radii of the sphere $a/(b-d)$. Plot parameters: $b = 1$ m, $d = 0.3$ m, $\omega = 200\pi$ rad/sec, $\omega_0 = 200\pi$ rad/sec, $Q = 10^5$ V/m.

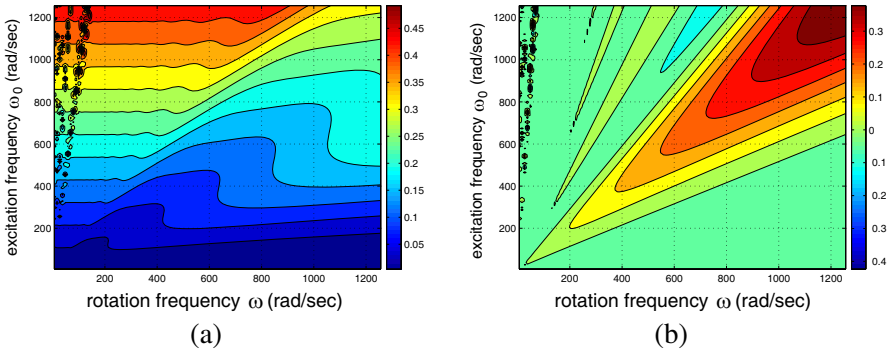


Figure 5. The: (a) RMS value U_{rms} and (b) DC component U_{dc} of the induced voltage (in V) in contour plot with respect to the rotation frequency of the loop ω and the excitation frequency of the incident wave ω_0 . Plot parameters: $b = 1$ m, $a = 1/3$ m, $d = 1/3$ m, $\xi = \pi/4$ rad, $Q = 10^5$ V/m.

This chaotic behavior is attributed to the fact that, in case $\omega \rightarrow 0$, the magnetic flux is considerably affected even by the slightest time variation in the frequency of the alternating field. In Fig. 5(b), the DC offset U_{dc} is represented for the same set of parameters. Note

that in all the previous examples, the presence of the scatterer makes the produced oscillating voltage to have nonzero average value which possesses similar waveforms with U_{rms} . This is not the case; when ω is chosen close to ω_0 , there is a substantial increase for growing frequencies.

4. CONCLUSION

In this work, we examine the induction of electromagnetic voltage across a rotating circular loop, in the presence of an eccentric metallic sphere under a low-frequency, plane-wave excitation. Similar topics combining two fundamental phenomena in electromagnetics (induction and scattering) have not been examined again. The variation of the measured output is represented as function of the sphere's characteristic parameters and several conclusions are drawn describing its effect on the magnetic flux through the coil. An interesting expansion of the present paper would be to assume a moving spherical scatterer affecting the time-dependent developed voltage and giving it certain desirable characteristics. Also, closed wires of arbitrary curvature rotating around arbitrary axes could be also investigated with use of similar techniques.

REFERENCES

1. Vaseghi, B., N. Takorabet, and F. Meibody-Tabar, "Transient finite element analysis of induction machines with stator winding turn fault," *Progress In Electromagnetics Research*, PIER 95, 1–18, 2009.
2. Sun, X. Y. and Z.-P. Nie, "Vector finite element analysis of multicomponent induction response in anisotropic formations," *Progress In Electromagnetics Research*, PIER 81, 21–39, 2008.
3. Hwang, S. M., J. I. Hong, and C. S. Huh, "Characterization of the susceptibility of integrated circuits with induction caused by high power microwaves," *Progress In Electromagnetics Research*, PIER 81, 61–72, 2008.
4. Nesterenko, M. V., D. Y. Penkin, V. A. Katrich, and V. M. Dakhov, "Equation solution for the current in radial impedance monopole on the perfectly conducting sphere," *Progress In Electromagnetics Research B*, Vol. 19, 95–114, 2010.
5. Valagiannopoulos, C. A., "An overview of the Watson transformation presented through a simple example," *Progress In Electromagnetics Research*, PIER 75, 137–152, 2007.

6. Alexopoulos, A., "Scattering cross section of a meta-sphere," *Progress In Electromagnetics Research Letters*, Vol. 9, 85–91, 2009.
7. Valagiannopoulos, C. A., "Single-series solution to the radiation of loop antenna in the presence of a conducting sphere," *Progress In Electromagnetics Research*, PIER 71, 277–294, 2007.
8. Coxeter, H. S. and S. L. Greitzer, *Geometry Revisited*, 8285, Mathematical Association of America, 1967.
9. Sadiku, M., *Elements of Electromagnetics*, 372, Oxford Series in Electrical and Computer Engineering, 2001.
10. Balanis, C. A., *Advanced Engineering Electromagnetics*, 924, John Wiley & Sons, 1989.
11. Wrede, R. C. and M. R. Spiegel, *Advanced Calculus*, 229–232, Schaumm's Outline Series, 2002.
12. Erma, V. A., "Exact solution for the scattering of electromagnetic waves from conductors of arbitrary shape. II. General case," *Physical Review*, 1544–1553, 1968.
13. Abramowitz, M. and I. A. Stegun, *Handbook of Mathematical Functions*, 437–438, National Bureau of Standards, 1970.